© 2022. Published by The Company of Biologists Ltd | Development (2022) 149, dev201213. doi:10.1242/dev.201213

RESEARCH ARTICLE

Translational control by maternal Nanog promotes oogenesis and early embryonic development

Mudan He[1,2,*], Shengbo Jiao[1,2,*], Ru Zhang[1,2], Ding Ye[1,2], Houpeng Wang[1,2] and Yonghua Sun[1,2,3,‡]

ABSTRACT

Many maternal mRNAs are translationally repressed during oocyte development and spatio-temporally activated during early embryogenesis, which is crucial for oocyte and early embryo development. By analyzing maternal mutants of *nanog* (M*nanog*) in zebrafish, we demonstrated that Nanog tightly controls translation of maternal mRNA during oogenesis via transcriptional repression of *eukaryotic translation elongation factor 1 alpha 1, like 2* (*eef1a1l2*). Loss of maternal Nanog led to defects of egg maturation, increased endoplasmic reticulum stress, and an activated unfold protein response, which was caused by elevated translational activity. We further demonstrated that Nanog, as a transcriptional repressor, represses the transcription of *eefl1a1l2* by directly binding to the *eef1a1l2* promoter in oocytes. More importantly, depletion of *eef1a1l2* in *nanog* mutant females effectively rescued the elevated translational activity in oocytes, oogenesis defects and embryonic defects of M*nanog* embryos. Thus, our study demonstrates that maternal Nanog regulates oogenesis and early embryogenesis through translational control of maternal mRNA via a mechanism whereby Nanog acts as a transcriptional repressor to suppress transcription of *eef1a1l2*.

KEY WORDS: Translational control, Oogenesis, Nanog, Zebrafish, Embryonic development

INTRODUCTION

During oocyte development, many maternal mRNAs are transcribed and accumulated, and temporal and spatial regulation of translational activation or repression of maternal mRNA determines oocyte development, maturation and early embryogenesis. Translation of many maternal mRNAs is repressed during oocyte development (Evans and Hunter, 2005; Piqué et al., 2008; Gosden and Lee, 2010), and maintenance of translational arrest of maternal mRNA is essential for normal oocyte development and maturation (Richter and Lasko, 2011; Yarunin et al., 2011). Failure of translational repression of maternal mRNAs leads to various developmental defects, including apoptosis of oocytes, impaired oocyte maturation and unsuccessful early embryonic development (Kotani et al., 2013; Takahashi et al., 2014; Miao et al., 2017; Petrachkova et al., 2019).

Various mechanisms of translational control have been described using different animal models. In zebrafish, the RNA-binding protein Zar1 binds to zona pellucida (ZP) mRNAs and represses translation of the ZP genes during oogenesis, and loss of Zar1 induces oocyte apoptosis and ovary degeneration (Miao et al., 2017). The RNA-binding protein Ybx1 associates with processing body components and represses global translation activity during early embryogenesis (Sun et al., 2018). In *Drosophila*, translation of many germ cell-specific mRNAs is repressed by RNA-binding proteins during oocyte maturation. The germline RNAs, *oskar* and *pgc*, are targeted by Bruno 1 or Pumilio at the 3′-untranslated region and translationally repressed during oogenesis, and mutations of the RNA-binding sites results in precocious translation and mislocalization of the mRNA (Kim-Ha et al., 1995; Snee et al., 2008; Flora et al., 2018). Me31B mediates translational silencing of both maternal mRNAs during the maternal-to-zygotic transition (MZT) and oocyte-localizing RNAs during transport to the oocyte (Nakamura et al., 2001; Wang et al., 2017). During transport of *nanos* mRNA to the oocyte, failure of translational repression of *nanos* mRNA by Smaug results in ectopic translation of *nanos* and defects of anteroposterior axis formation (Dahanukar and Wharton, 1996; Smibert et al., 1996, 1999). To date, the studies of translational repression in oogenesis have focused mainly on post-transcriptional regulation, in which the translational repressors are mainly RNA-binding proteins. It remains unknown whether there is a general translational repressor that regulates the translation of maternal mRNAs at a global level in oocytes.

Nanog is known for its prominent function as a regulator of pluripotency in embryonic stem cells (Mitsui et al., 2003; Boyer et al., 2005; Loh et al., 2006) and reprogramming of somatic cells to the pluripotent state (Takahashi and Yamanaka, 2006; Silva et al., 2009). In zebrafish, Nanog has been shown to be a transcriptional activator that plays a central role in regulating early embryogenesis. For instance, maternal Nanog mediates endoderm formation through Mxtx2-Nodal signaling (Xu et al., 2012), and is required for both extra-embryonic development (Gagnon et al., 2018) and embryonic architecture formation (Veil et al., 2018). During the MZT, the maternally provided transcription factors Pou5f3, SoxB1 and Nanog open up chromatin in a coordinated manner to initiate zygotic genome activation (ZGA) (Lee et al., 2013; Veil et al., 2019; Pálfy et al., 2020). Our recent study shows that Nanog suppresses the global activation of maternal β-catenin activity to safeguard dorsal-ventral axis formation (He et al., 2020). However, as a strongly maternally expressed gene, the role of Nanog in oogenesis is still unknown.

In this study, we found that the absence of maternal *nanog* leads to various developmental defects in oocytes and early embryos. Our study demonstrates that global translational activity is greatly enhanced in *nanog* mutant oocytes and maternal *nanog* mutant

[1]State Key Laboratory of Freshwater Ecology and Biotechnology, Institute of Hydrobiology, Innovation Academy for Seed Design, Chinese Academy of Sciences, Wuhan 430072, China. [2]College of Advanced Agricultural Sciences, University of Chinese Academy of Sciences, Beijing 100049, China. [3]Hubei Hongshan Laboratory, Wuhan 430070, China.
*These authors contributed equally to this work

‡Author for correspondence (yhsun@ihb.ac.cn)

M.H., 0000-0003-2018-9384; S.J., 0000-0002-8882-3313; R.Z., 0000-0002-1661-5638; D.Y., 0000-0003-3460-1122; H.W., 0000-0002-7462-6562; Y.S., 0000-0001-9368-6969

Handling Editor: Swathi Arur
Received 16 August 2022; Accepted 9 November 2022

Development (2022) 149, dev201213. doi:10.1242/dev.201213

(M*nanog*) embryos, as a result of the transcriptional activation of *eukaryotic translation elongation factor 1 alpha 1, like 2* (*eef1a1l2*) during oocyte development and maturation. We further show that maternal depletion of *eef1a1l2* significantly rescues the developmental defects of *nanog* mutant oocytes and early development of M*nanog* embryos. Thus, our study reveals a role for Nanog as a general translational repressor through transcriptional repression of *eef1a1l2* in zebrafish oogenesis.

RESULTS

Maternal *nanog* is required for oocyte maturation and early embryonic development

We previously generated a *nanog* mutant using transcription activator-like effector nuclease (TALEN) technology and addressed its crucial role in regulating dorsal formation by interfering with TCF factors (He et al., 2015, 2020). Here, by analyzing the phenotype of maternal mutant of M*nanog* embryos, we found that the M*nanog* embryos showed slow epibolic movement, resulting in the accumulation of blastomere cells at the animal pole at gastrulation stage (Fig. 1A), which is similar to the phenotype of the maternal and zygotic mutant of *nanog* (MZ*nanog*) (He et al., 2020). Comparison of the size of M*nanog* and wild-type (WT) embryos at 15 min post-fertilization (mpf) revealed that the M*nanog* embryos had significantly smaller chorion diameter and oocyte diameter than did WT embryos (Fig. 1B-D). In addition, we analyzed the activation phenotype of mutant eggs by monitoring cortical granule (CG) exocytosis and cytoplasmic streaming. Fluorescein-conjugated *Maclura pomifera* lectin was used to label CGs to assess CG exocytosis in activated eggs. Compared with WT eggs, *nanog* mutant eggs showed many retained CGs (Fig. 1E) at 10 min post-activation (mpa). CellTracker CM-DiI Dye was injected into the yolk of M*nanog* and WT embryos to monitor cytoplasmic streaming. In WT embryos, vigorous cytoplasmic movement towards the animal pole was recorded (Movie 1). In contrast, M*nanog* embryos showed sluggish cytoplasmic streaming (Movie 2). These results indicate that maternal Nanog is essential for egg activation and early embryonic development.

Moreover, terminal deoxynucleotidyl transferase dUTP nick end labeling (TUNEL) revealed apoptotic signals in Balbiani bodies and the cytoplasm of early-stage mutant oocytes, but not in WT oocytes (Fig. S1A). Mitochondria are enriched in the Balbiani body and also present throughout the oocyte cytoplasm (Marlow and Mullins, 2008; Jamieson-Lucy and Mullins, 2019); thus, *nanog* deficiency induced the mitochondrial apoptosis during oocyte development.

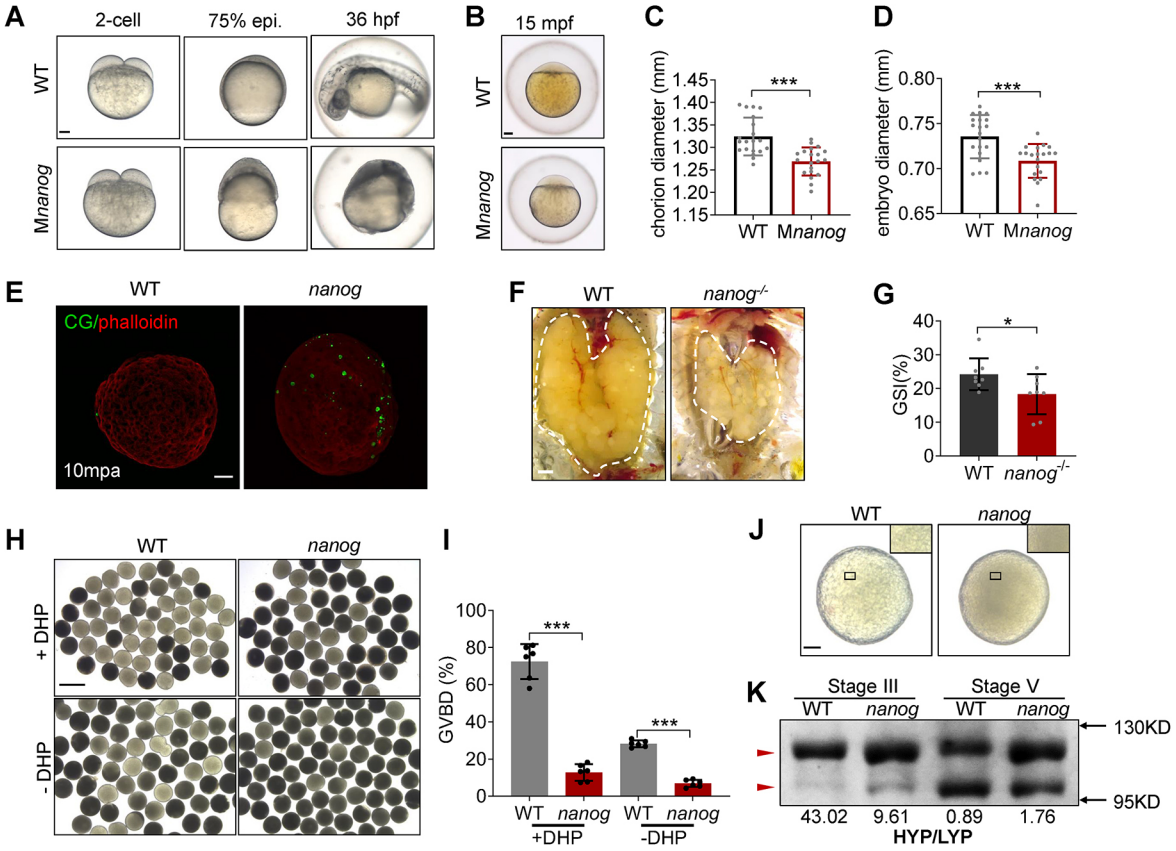

Fig. 1. Loss of maternal *nanog* results in oocyte maturation defects. (A) Bright-field images showing the embryonic malformation of M*nanog* mutants in contrast to time-matched WT embryos. Scale bar: 100 µm. (B) WT and M*nanog* embryos with chorions at 15 mpf. Scale bar: 100 µm. (C,D) Measurement of chorion diameter and oocyte diameter at 15 mpf. ***P<0.001. n=20. (E) Representative images showing labeling of CGs in WT and *nanog* mutant eggs fixed at 10 mpa. F-actin was stained using phalloidin to show the outline of embryo. Scale bar: 100 µm. n=25. (F) Appearance of ovaries (outlined) dissected from WT and *nanog*$^{-/-}$ females. Scale bar: 1 mm. (G) The GSI of WT and *nanog*$^{-/-}$ females. n=8. *P<0.05. (H) Morphology of stage IV follicles dissected from WT and *nanog*$^{-/-}$ ovaries with or without incubation in DHP (1 µg/ml) for 2 h. Scale bar: 1 mm. (I) Comparison of the GVBD percentage in WT and *nanog* mutant follicles. Six fish of each group were analyzed. (J) Stage V follicles from WT and *nanog* mutant. Insets show enlarged regions of the yolk and relative opaqueness is seen in *nanog* mutants. Scale bar: 100 µm. (K) SDS-PAGE and Coomassie staining of major yolk proteins of stage III and stage V follicles. The higher and lower molecular weight yolk proteins (HYP and LYP) are indicated by the red arrowheads. HYP/LYP ratios were calculated (shown underneath) to represent yolk protein cleavage levels.

Development (2022) 149, dev201213. doi:10.1242/dev.201213

Robust active-Caspase3 signals were also detected in M*nanog* embryos, but not WT embryos, at 75% epiboly stage (Fig. S1B). These data demonstrate that *nanog* depletion induces oocyte apoptosis and the death of early embryonic cells.

Through morphological and histological analyses, we found that the gonadosomatic index (GSI; gonad weight/body weight×100%) was significantly reduced in *nanog*$^{-/-}$ compared with WT females (Fig. 1F,G), indicating defects of oocyte development in *nanog* mutants. To characterize further the oocyte maturation defects in the *nanog* mutant, stage IV follicles (follicle-enclosed oocytes) were isolated and treated with (or without) 17α,20β-dihydroxy-4-pregnen-3-one (DHP) to determine the percentage of germinal vesicle breakdown (GVBD) *in vitro*. After 2 h incubation, the percentage of GVBD in *nanog* mutant follicles was 6.9% without DHP treatment, which is significantly lower than that in WT follicles (28.2%) (Fig. 1H,I). Even when treated with DHP, the percentage of GVBD in *nanog* mutant follicles was as low as 12.8%, which is also significantly lower than that in WT follicles (72.4%) (Fig. 1H,I). Moreover, the *nanog* mutant stage V follicles were less transparent than those of WT (Fig. 1J). During oocyte maturation, the major yolk proteins undergo cleavage and change the appearance of the oocyte from opaque to transparent (Dosch et al., 2004). Therefore, we compared the composition of higher and lower molecular weight yolk proteins (HYP and LYP) from stage III and stage V follicles to evaluate the yolk protein cleavage level. In stage III follicles, the HYP/LYP ratio were even lower in the *nanog* mutant than in WT, whereas the ratio was greatly decreased in WT stage V follicles than in mutants (Fig. 1K). These results suggested the deficiency of yolk protein cleavage during maturation of *nanog* mutant oocytes. In addition, we also generated a transgenic line, *Tg*(*CMV:nanog-myc*), in a *nanog* homozygous background. Immunofluorescence staining using anti-Myc antibody showed that Nanog is strongly expressed in early oocytes (Fig. S1C). Moreover, this overexpression of *nanog* could rescue the early developmental defects of M*nanog* (Fig. S1D), demonstrating that oocyte maturation and early embryonic defects were caused by deficiency of Nanog. Therefore, we conclude that loss of maternal *nanog* leads to pleiotropic defects of oogenesis and early embryonic development.

Loss of maternal *nanog* elevates the global translation level

In order to understand the molecular mechanism of oogenesis regulation by Nanog, we quantitatively compared the proteomes of *nanog* mutant eggs with WT using isobaric tags for relative and absolute quantitation (iTRAQ) technology. More than 1600 proteins were identified in eggs from the two genotypes. These proteins were classified using the COG (Clusters of Orthologous Groups of proteins) database, and two of the top categories identified were protein translation-related biological processes (cluster J and O) (Fig. S2A). Comparing the mutant with WT, 67 proteins showed differential expression (P<0.05) (Table S1), and 39 proteins were increased in mutant eggs (Fig. S2B). Gene ontology analysis of the upregulated proteins showed that one of the most significant enriched biological processes was translation elongation factor activity (Fig. S2C). Gene-Concept Network analysis revealed that four elongation factors were enriched (Fig. S2D). These results indicate that global translation activity is elevated in *nanog*-deficient eggs.

To verify this speculation, we assessed the translation activity of M*nanog* embryos at an early developmental stage. The mCherry reporter mRNA was injected into one-cell-stage WT and M*nanog* embryos together with the same amount of GFP protein. The injected embryos were imaged under a fluorescence microscope at later stages and fluorescence levels were measured. The GFP protein acted as the loading control for injection. Fluorescence measurement showed that the reporter mRNA translation level was significantly higher in M*nanog* embryos (Fig. 2A,B). Western blot analysis confirmed the increase of mCherry reporter translation in M*nanog* embryos (Fig. 2C,D). We then treated the stage IV mutant follicles with an eIF4E/eIF4G interaction inhibitor, 4EGI-1, which has been shown to block translation initiation by disruption of the eIF4E/eIF4G association by binding to eIF4E (Moerke et al., 2007), and determined the percentage of GVBD *in vitro*. After 2 h incubation with 4EGI-1, the percentage of GVBD in *nanog* mutant follicles was remarkably increased from 10.4% to 28.3% with DHP treatment, and increased from 8.3% to 15.2% without DHP treatment (Fig. S2E,F). Taken together, these results suggest that Nanog is necessary for repressing the global translation of maternal mRNAs during oogenesis and early embryonic development.

Nanog depletion triggers ER stress and the unfolded protein response (UPR)

The ER functions as a crucial machinery for protein synthesis, modification and trafficking in eukaryotic cells. Under ER stress, cells activate the UPR to alleviate ER burden by reducing protein translation, increasing protein degradation and generating additional chaperones to assist protein folding. Therefore, ER stress and the UPR are often associated with aberrant translational derepression (Kaufman, 2002; Miao et al., 2017). The UPR functions through three major pathways, initiated by three ER-localized transmembrane proteins in mammals: protein kinase RNA-like ER kinase (PERK), activating transcription factor 6 (ATF6) and inositol-requiring enzyme 1 (IRE1), to maintain ER homeostasis (Hetz, 2012). Normally, the N termini of these transmembrane ER proteins are held by the ER chaperone Hspa5 (also termed Grp78 or Bip), preventing their aggregation. When misfolded proteins accumulate, Hspa5 releases the proteins, allowing aggregation of these transmembrane signaling proteins, and launching the UPR (Rao and Bredesen, 2004; Shen et al., 2004; Schröder and Kaufman, 2005). Activation of PERK upregulates the expression of CCAAT-enhancer-binding protein homologous protein (CHOP), which induces cell apoptosis and death (Oyadomari and Mori, 2004; Iurlaro and Muñoz-Pinedo, 2016). We detected the transcriptional level and protein level of *hspa5* and the CHOP-encoding gene *ddit3* in *nanog* mutant ovary, found that both transcription and translation of *hspa5* and *ddit3* are increased in *nanog*$^{-/-}$ ovary (Fig. 2E-G). The TUNEL assay also revealed an obvious apoptosis signal in mutant ovary (Fig. S1A). Owing to the lack of specific antibodies against zebrafish ATF6 and IRE1A, we detected the mRNA expression of *atf6* and *ire1a* (*ern1*), and discovered that both of *atf6* and *ire1a* expression were increased in *nanog* mutant ovary (Fig. 2H,I). Given that phosphorylated ribosomal protein S6 (pS6) is considered an indicator of active protein synthesis (Biever et al., 2015; Meyuhas, 2015), we also detected the expression level of total S6 and pS6, and found that the pS6 level was significantly increased in *nanog* mutant ovary (Fig. 2J,K). Finally, we used PERK inhibitors (GSK2606414 and ISRIB) to treat *nanog* mutant and WT follicles and determined the occurrence of GVBD. After treatment with the two inhibitors, the GVBD percentage in mutant follicles significantly recovered (Fig. 2L,M). These results demonstrate that loss of *nanog* triggers ER stress and UPR and thus leads to failure of oocyte development and maturation.

Development (2022) 149, dev201213. doi:10.1242/dev.201213

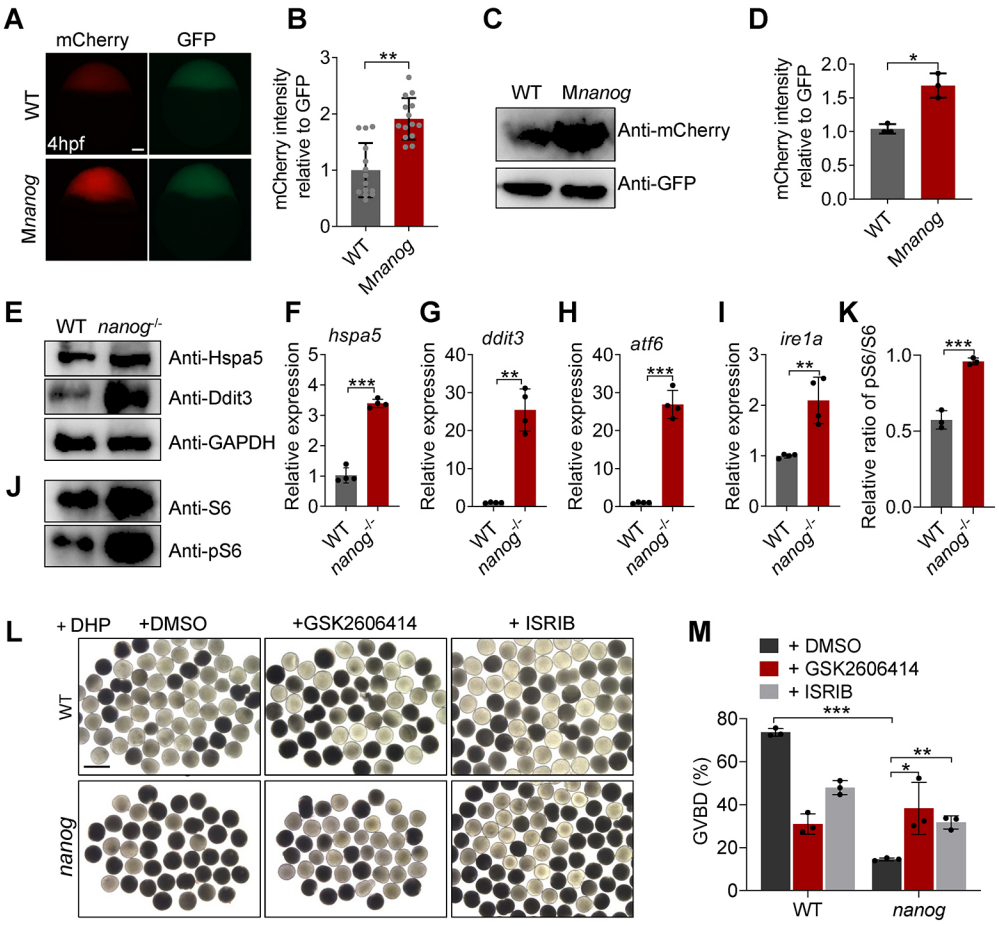

Fig. 2. Loss of *nanog* triggers ER stress and UPR and elevates global translation activity. (A) Fluorescent images showing mCherry reporter levels with GFP protein control levels in WT and M*nanog* embryos at 4 hpf. Scale bar: 100 µm. (B) Measurement of mCherry reporter intensities relative to GFP. $^{**}P$<0.01. *n*=14. (C,D) Western blotting analysis of mCherry reporter levels at 4 hpf. $^{*}P$<0.05. (E) Western blot analysis of Hspa5 and Ddit3 in WT and *nanog*$^{-/-}$ ovaries. (F-I) RT-qPCR analysis of *hsp5a* (F), *ddit3* (G), *atf6* (H) and *ire1a* (I) in WT and *nanog*$^{-/-}$ ovaries. $^{**}P$<0.01, $^{***}P$<0.001. *n*=4. (J) Western blot analysis of S6 and phosphorylated S6 in WT and *nanog*$^{-/-}$ ovaries. The internal control of GAPDH is shown in E. (K) Statistical analysis of phosphorylated S6/S6 ratio shown in J. $^{***}P$<0.001. (L) Morphology of stage IV follicles dissected from WT and *nanog*$^{-/-}$ ovaries and treated with two different PERK inhibitors for 2 h. Follicles dissected from three fish were treated with inhibitors for 2 h (all in the presence of DHP). Final concentrations: GSK2606414, 50 nM; ISRIB, 5 µM; DHP, 1 µg/ml. Scale bar: 1 mm. (M) Comparison of GVBD percentage in WT and *nanog* mutant follicles treated with or without PERK inhibitor. *n*=3. $^{*}P$<0.05, $^{**}P$<0.01, $^{***}P$<0.001.

Loss of maternal Nanog upregulates *eef1a1l2* transcription level

To find out the molecular mechanism responsible for Nanog regulating translation activity in early embryos, we conducted RNA-sequencing (RNA-seq) analysis to compare *nanog* mutant eggs and WT eggs. A total of 137 genes were differentially expressed in mutant and WT eggs, with 74 upregulated genes and 63 downregulated genes in mutant eggs. Among the upregulated genes, *eukaryotic elongation factor 1 alpha 1, like 2* (*eef1a1l2*) was one of the most significantly differentially expressed (Fig. 3A). eEF1A1l2 is a major subunit of the translation elongation factor 1 complex (eEF1), which plays a central role in protein synthesis by delivering aminoacyl-tRNAs to the elongating ribosome (Sasikumar et al., 2012). Calculation of reads per kilobase of exon per million reads mapped (RPKM) and visualization of RNA-seq reads mapped to the *eef1a1l2* showed significant upregulation of *eef1a1l2* in mutant eggs (Fig. S3A,B). Reverse-transcription quantitative PCR (RT-qPCR) further supported the suggestion that the transcription of *eef1a1l2* was significantly increased in *nanog* mutant follicles at five different stages and in early embryonic developmental stages (Fig. 3B, Fig. S3C). *In situ* hybridization of ovary cryosection also showed increased expression of *eef1a1l2* in the *nanog* mutant (Fig. 3C). In contrast, transgenic overexpression of *nanog* significantly decreased the high expression levels of *eef1a1l2* in mutant oocytes (Fig. 3B,C). These data indicate that *nanog* deficiency leads to strong transcriptional activation of *eef1a1l2* during oocyte development and maturation.

To verify the transcriptional inhibition of *eef1a1l2* by Nanog, WT *nanog* or a constitutive repressor type *nanog* (Engrailed fusion with Nanog homeodomain, En-*nanog*) (He et al., 2020) was overexpressed and *eef1a1l2* transcription was measured at shield stage. Both *in situ* hybridization and RT-qPCR analysis showed that the expression of *eef1a1l2* was significantly reduced in both *nanog* and En-*nanog* overexpressing embryos (Fig. 3D,E), suggesting that Nanog acts as a transcriptional repressor on the regulation of *eef1al2*. To clarify whether Nanog directly binds to the promoter region of *eef1a1l2* to repress its transcription, a chromatin immunoprecipitation (ChIP) assay was conducted. Ovaries of *Tg*(CMV:*nanog-myc*) at 6 mpf were dissected and ChIP was performed using an anti-Myc antibody. The precipitated chromatin was then analyzed by PCR using primer pairs that could amplify fragments of *eef1a1l2* promoter. A fragment of the *rpl5b* exon amplified by a specific primer pair was used as control (Belting et al., 2011). As shown in Fig. 3F, the promoter fragment of *eef1a1l2* was significantly enriched in the immunoprecipitated sample with no enrichment of the control genomic region *rpl5*. Thus, this result demonstrates that Nanog directly binds to the promoter of *eef1a1l2* to inhibit its transcription. All these data illustrate that Nanog directly inhibits the transcription of *eef1a1l2* and that depletion of *nanog* leads to significantly increased expression of *eef1a1l2*.

Deficiency of eEF1A1l2 ameliorates impaired oogenesis of *nanog* mutants

We then generated a homozygous mutant of *eef1a1l2* and two types of *eef1a1l2* mutants were obtained (Fig. S4A); neither of the two

Development (2022) 149, dev201213. doi:10.1242/dev.201213

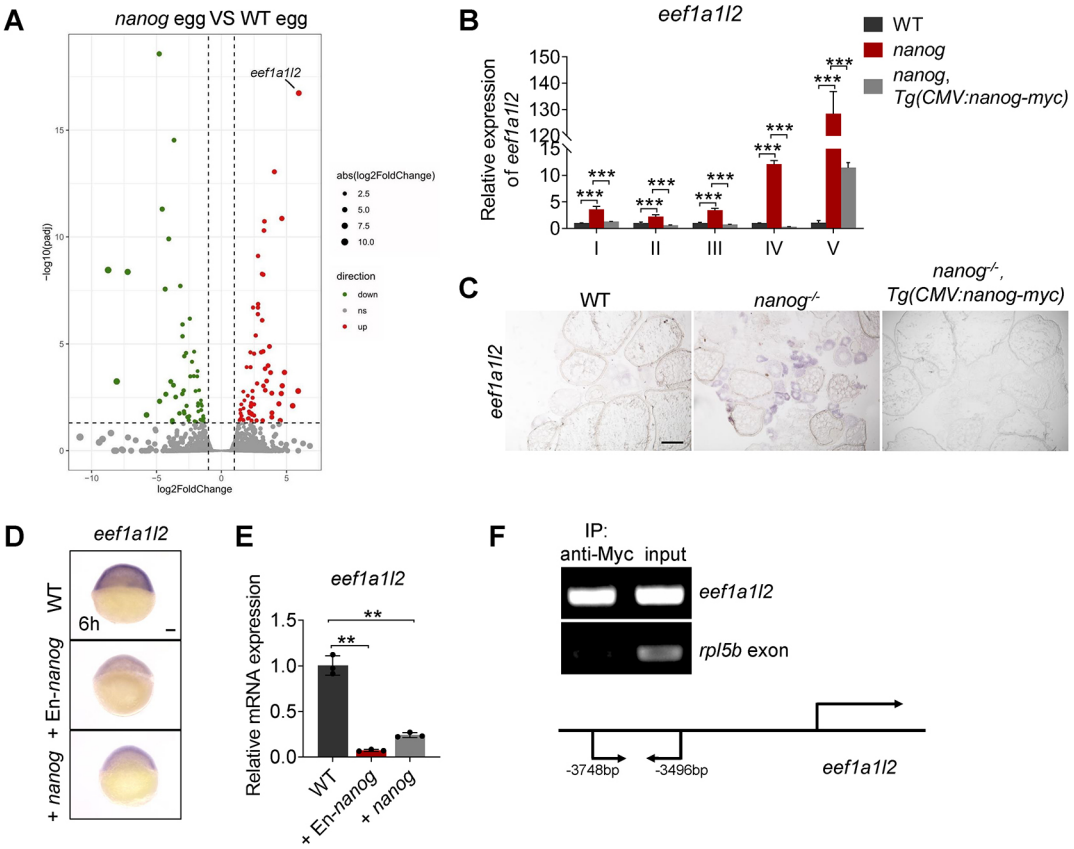

Fig. 3. Nanog transcriptionally inhibits the expression of *eef1a1l2*. (A) RNA-seq analysis showing significantly increased expression of *eef1a1l2* in *nanog* null eggs. Red dots indicate upregulated genes, green dots indicate downregulated genes, and gray dots indicate genes that were not differentially expressed in *nanog* mutant eggs. (B) Detection of *eef1a1l2* expression in *nanog* mutant oocytes at different stages revealed by RT-qPCR. ***P<0.001. n=3. (C) Detection of *eef1a1l2* expression in ovaries of WT, *nanog* mutant, and *Tg*(*CMV:nanog-myc*) in *nanog* mutant background by *in situ* hybridization on cryosections. Scale bar: 200 µm. (D,E) WISH (D) and RT-qPCR (E) analysis showed reduced expression of *eef1a1l2* in *nanog* or En-*nanog* overexpressed embryos at 6 hpf. Images in D are representative of 36/36 embryos for WT, 38/39 for +EN-nanog and 32/32 for +nanog. **P<0.01. n=3. Scale bar: 100 µm. (F) ChIP analysis of *Tg*(CMV:*nanog-myc*) ovaries with anti-Myc antibody at 6 months post-fertilization. The promoter region of *eef1a1l2* was enriched in precipitated chromatin. *rpl5b* served as a negative control. Schematic depicts the genomic sequence of *eef1a1l2*, and the sequence located between −3748 and −3496 bp upstream of the amplified region.

maternal and zygotic mutants of *eef1a1l2* showed obvious embryonic defects (Fig. S4B), and we used the *ihb99* allele for subsequent study. To determine whether Nanog promotes oocyte development and maturation through suppression of *eef1a1l2*, we generated a double homozygous mutant of *nanog* and *eef1a1l2* and studied whether depletion of *eef1a1l2* could ameliorate the oogenesis defect of *nanog* mutant. By morphological analysis, we found that the double maternal mutant of *nanog* and *eef1a1l2* (M*nanog*, M*eef1a1l2*) showed increased embryo chorion diameter and oocyte diameter at 15 mpf, compared with M*nanog* embryos, whereas the single maternal mutant of *eef1a1l2* (M*eef1a1l2*) showed no difference in embryo chorion diameter and oocyte diameter compared with WT (Fig. 4A-C). The process of CG exocytosis in double mutant eggs (*nanog*,*eef1a1l2*) were also comparable to WT at 10 mpa, which showed fewer retained CGs than the *nanog* mutant (Fig. 4D). Moreover, cytoplasmic streaming labeled by CM-DiI dye in the double maternal mutant embryo (M*nanog*, M*eef1a1l2*) showed vigorous cytoplasmic movement, similar to the WT (compare Movie 1 and Movie 3). These results indicate that depletion of *eef1a1l2* rescues the egg activation defect of *nanog* mutant.

Therefore, we further examined the oocyte development and maturation improvement in the double mutant. Morphologically, The GSI was increased in double mutant (*nanog*$^{-/-}$,*eef1a1l2*$^{-/-}$) females, compared with *nanog*$^{-/-}$ females (Fig. 4E,F). The double-mutant stage V follicles were more transparent than the *nanog* mutant, similar to WT (Fig. 4G). The altered HYP/LYP ratio in stage III and stage V follicles in the double mutant confirmed this conclusion (Fig. 4H). The GVBD percentage was also remarkably increased in double-mutant follicles (Fig. 4I,J). The *eef1a1l2* single mutant showed no obvious defects in oogenesis (Fig. 4A-C,E-G,I,J) or embryogenesis (Fig. S4B), so we did not analyze *eef1a1l2*$^{-/-}$ in subsequent experiments. These results together indicate that Nanog promotes oogenesis by suppressing the expression of *eef1a1l2* in the oocyte.

Given the role of eEF1A1l2 in translation elongation, we further investigated the rescue effect of overactivated translation in the double mutant. Previous studies have shown that translation of Cyclin B1 should be repressed in immature oocytes (Vardy and Orr-Weaver, 2007; Kotani et al., 2013; Takahashi et al., 2014), and translation of ZP proteins is also repressed during oogenesis (Miao et al., 2017). Therefore, we detected the translation level of Cyclin B1 and Zp3b in WT, *nanog* mutant, and *nanog* and *eef1a1l2* double-mutant immature follicles (stage I/II). The result showed that the translation of Cyclin B1 and Zp3b was silent in WT immature oocyte, but the protein levels of Cyclin B1 and Zp3b were significantly increased in the immature oocyte of the *nanog* mutant, indicating that the translation level is elevated in the *nanog* mutant.

Development (2022) 149, dev201213. doi:10.1242/dev.201213

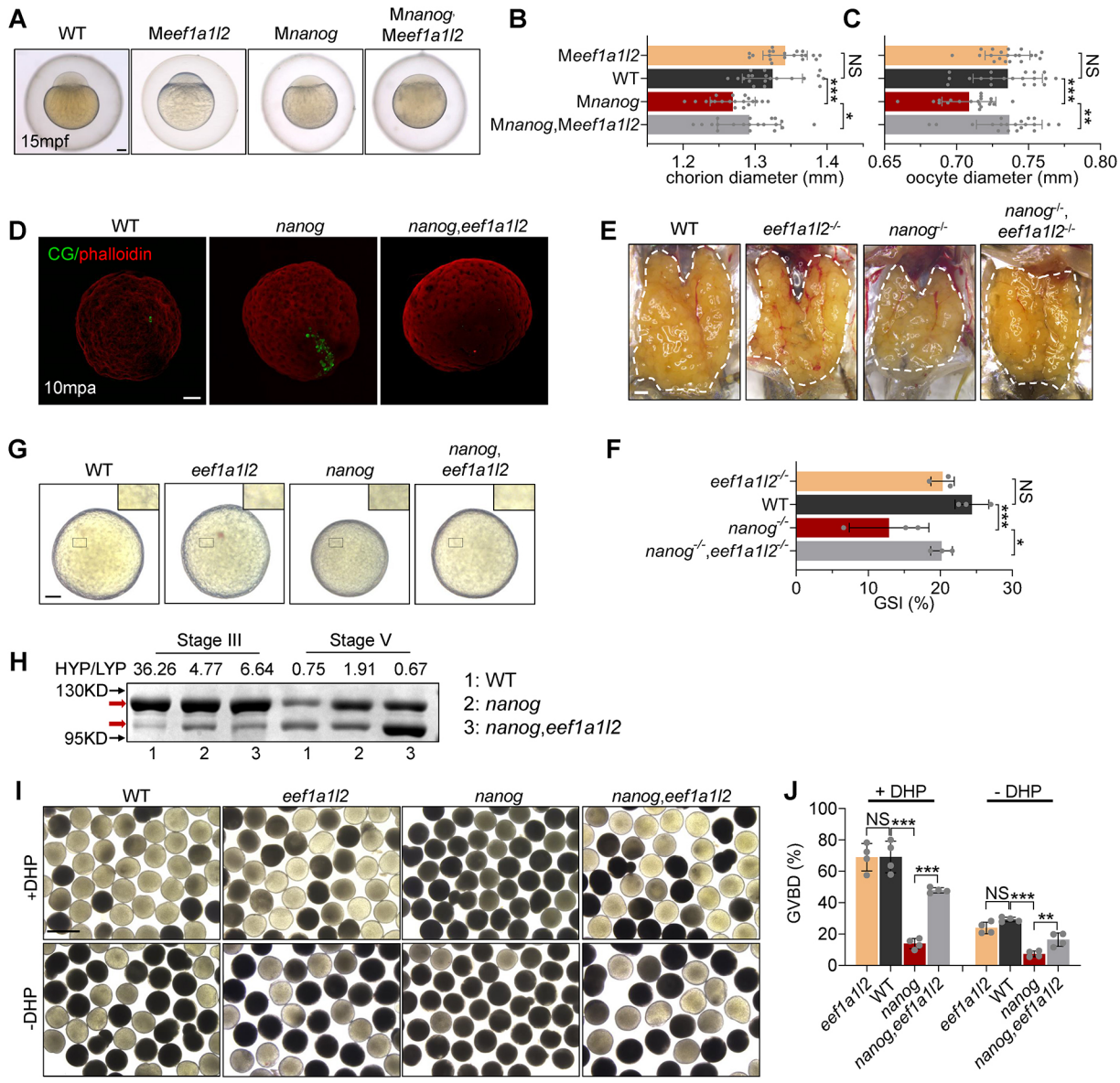

Fig. 4. Depletion of *eef1a1l2* rescues impaired oocyte maturation of the *nanog* mutant. (A) WT, M*eef1a1l2*, M*nanog* and M*nanog*,M*eef1a1l2* embryos with chorions at 15 mpf. Scale bar: 100 µm. (B,C) Measurement of chorion diameters and oocyte diameters at 15 mpf. **P*<0.05, ****P*<0.001. NS, no significant difference. *n*=20. (D) Representative images showing labeling of CGs in WT, *nanog* and *nanog*,*eef1a1l2* double-mutant eggs fixed at 10 mpa. F-actin was stained using phalloidin to show the outline of the embryo. *n*=15. Scale bar: 100 µm. (E) Appearance of ovaries (outlined) dissected from WT, *eef1a1l2*$^{-/-}$, *nanog*$^{-/-}$ and *nanog*$^{-/-}$,*eef1a1l2*$^{-/-}$ females. Scale bar: 1 mm. (F) GSI of WT, *eef1a1l2*$^{-/-}$, *nanog*$^{-/-}$ and *nanog*$^{-/-}$,*eef1a1l2*$^{-/-}$ females. *n*=3. **P*<0.05, ****P*<0.001. NS, no significant difference. (G) Morphology of stage V follicles from WT, *eef1a1l2*$^{-/-}$, *nanog*$^{-/-}$ and *nanog*$^{-/-}$,*eef1a1l2*$^{-/-}$. Insets show enlarged regions of the yolk. Scale bar: 100 µm. (H) SDS-PAGE and Coomassie staining of major yolk proteins of stage III and stage V follicles. The higher and lower molecular weight yolk proteins (HYP and LYP) are indicated by red arrows. HYP/LYP ratios (shown above) were calculated to represent yolk protein cleavage levels. (I) Morphology of stage IV follicles dissected from WT, *eef1a1l2*$^{-/-}$, *nanog*$^{-/-}$ and *nanog*$^{-/-}$,*eef1a1l2*$^{-/-}$ ovaries with or without DHP (1 µg/ml) incubation for 2 h. Scale bar: 1 mm. (J) Comparison of the GVBD percentage in WT, *eef1a1l2*$^{-/-}$, *nanog*$^{-/-}$ and *nanog*$^{-/-}$,*eef1a1l2*$^{-/-}$ follicles. ***P*<0.01, ****P*<0.001. NS, no significant difference. *n*=4.

However, this increased translation level could be restored by deletion of *eef1a1l2* in the *nanog* mutant (Fig. S5A-D). In addition, mCherry mRNA reporter and GFP protein were co-injected at the one-cell stage in WT, M*nanog*, and M*nanog*,M*eef1a1l2* embryos. The fluorescence intensity of mCherry was measured at 4 h post-fertilization (hpf). Fluorescence measurement showed that the reporter translation level was significantly reduced in M*nanog*, M*eef1a1l2* embryos (Fig. S5E,F). These results indicate that Nanog controls the translation of maternal mRNAs by inhibiting the transcription of *eef1a1l2*.

Depletion of *eef1a1l2* alleviates ER stress and UPR in *nanog* mutant oocytes

Because depletion of *eef1a1l2* ameliorates the oogenesis defect of the *nanog* mutant, we wondered whether eEF1A1l2 depletion alleviates ER stress. We examined the mRNA expression level of ER stress-associated genes, and found that the increased expression of *hspa5*, *ddit3*, *atf6* and *ire1a* in *nanog* mutant ovary were all restored in the *nanog* and *eef1a1l2* double mutant (Fig. 5A-D). IRE1 is a unique RNase that removes an internal 26 nucleotides from X-box binding protein 1 (*xbp1*) mRNA transcripts in the

Development (2022) 149, dev201213. doi:10.1242/dev.201213

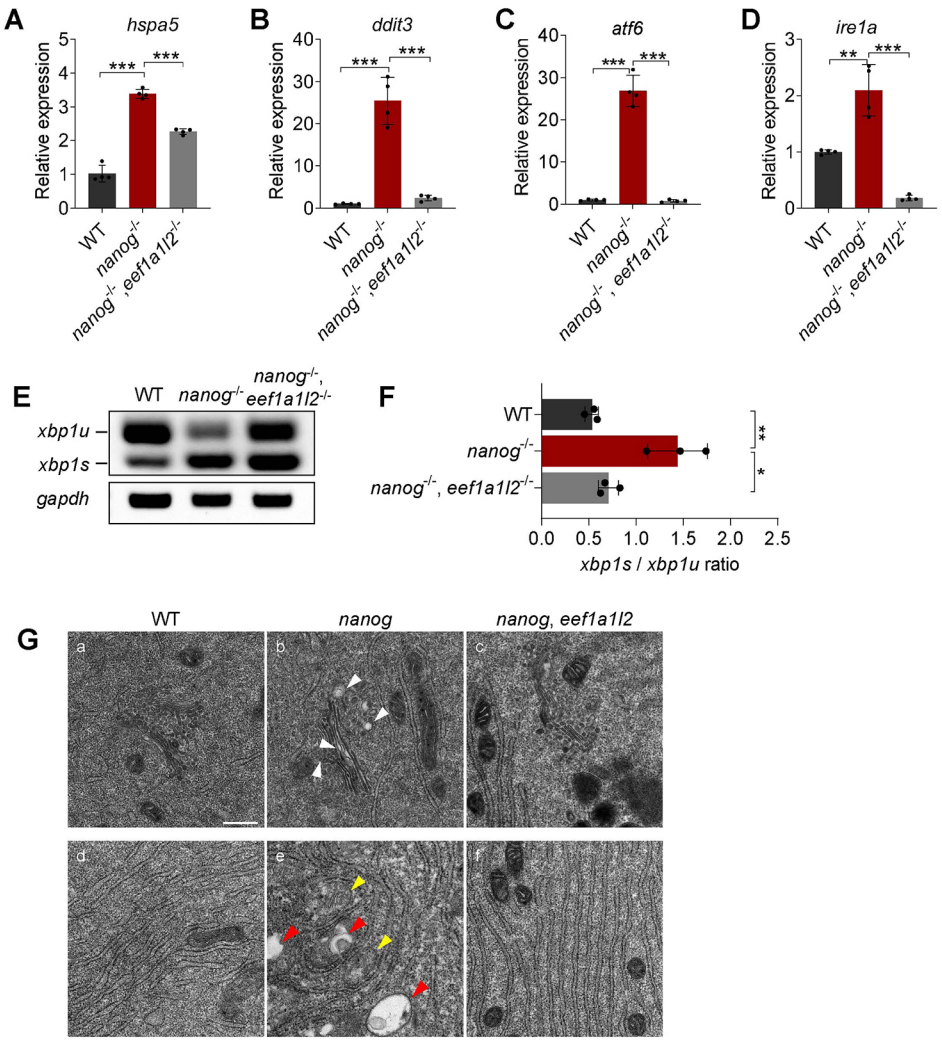

Fig. 5. Depletion of *eef1a1l2* ameliorates ER stress and UPR in *nanog* mutant oocytes. (A-D) RT-qPCR analysis showing decreased expression of *hspa5* (A), *ddit3* (B), *atf6* (C) and *ire1a* (D) in *nanog* and *eef1a1l2* double-mutant ovaries, compared with *nanog* mutant ovaries. ***P*<0.01, ****P*<0.001. *n*=4. (E,F) RT-PCR examination of *xbp1* splicing. The ratio of spliced *xbp1* (*xbp1s*) mRNA to unspliced *xbp1* (*xbp1u*) mRNA was increased in *nanog* mutant ovaries, but restored in *nanog* and *eef1a1l2* double-mutant ovaries. *gapdh* was used as internal control. The *xbp1s*/*xbp1u* ratio in F represents the intensity ratio of the corresponding PCR product bands in E. **P*<0.05, ***P*<0.01. *n*=3. (G) ER, Golgi and mitochondria structure in WT, *nanog* mutant and double-mutant stage I oocytes as revealed by transmission electron microscopy. White arrowheads indicate Golgi apparatus, yellow arrowheads indicate mitochondria, red arrowheads indicate lysosomes. Scale bar: 0.5 µm.

cytoplasm and activates expression of genes involved in protein folding and degradation; thus, the splicing of *xbp1* mRNA has been established as a common indicator of ER stress (Shen et al., 2001; Yoshida et al., 2001; Li et al., 2015). We examined altered splicing of *xbp1* mutant and WT ovaries and discovered that the splicing ratio of *xbp1* was increased in *nanog* mutant ovary, and this excessive splicing was reduced in the double-mutant ovary (Fig. 5E,F).

To observe organelle changes that may accompany the response to ER stress, ultrastructure analysis using transmission electron microscopy (TEM) was performed WT, *nanog* mutant and double mutant stage I oocytes. WT oocytes showed normal morphology of ER, Golgi apparatus and mitochondria (Fig. 5Ga,Gd). However, *nanog* mutant oocytes exhibited disruption of the Golgi apparatus, including swelling of the Golgi apparatus, dilated and disintegrated vesicles, and collapse of the Golgi complex (Fig. 5Gb, white arrowheads). *nanog* mutant oocytes also showed incompact and swollen mitochondria (Fig. 5Ge, yellow arrowheads), as well as evident lysosome distribution (Fig. 5Ge, red arrowheads). In contrast, the *nanog* and *eef1a1l2* double mutant the structure of ER, Golgi apparatus and mitochondria was normal (Fig. 5Gc,Gf). These data demonstrate that depletion of *eef1a1l2* alleviates ER stress and UPR in the *nanog* mutant, indicating that transcriptional activation of *eef1a1l2* in *nanog* mutant oocytes induces ER stress and UPR, thus leading to defects of oogenesis.

Depletion of *eef1a1l2* rescues early embryonic development defects in the *nanog* mutant

Given that depletion of *eef1a1l2* rescues the oogenesis defect and alleviates ER stress and UPR in the *nanog* mutant, we wondered whether depletion of *eef1a1l2* would have a rescue effect on the early embryonic development defects. We examined the early embryonic development phenotype of the double mutant. The morphological phenotypes of WT, M*nanog* (*nanog*$^{-/-}$ female cross with WT male), M*nanog*,M*eef1a1l2* (*nanog*$^{-/-}$,*eef1a1l2*$^{-/-}$ female cross with WT male), M*nanog*,MZ*eef1a1l2* (*nanog*$^{-/-}$,*eef1a1l2*$^{-/-}$ female cross with *eef1a1l2*$^{-/-}$ male), and M*nanog*,Z*eef1a1l2* (*nanog*$^{-/-}$,*eef1a1l2*$^{+/-}$ female cross with *eef1a1l2*$^{-/-}$ male; *nanog*$^{+/-}$,*eef1a1l2*$^{-/-}$ embryos were genotyped) were recorded at 0.2, 8, 12 and 24 hpf. As described in Fig. 1A, blastomere cells stacked at the animal pole and were unable to complete the gastrulation in M*nanog* embryos. Until 24 hpf, M*nanog* embryos still showed abnormal shapes and died gradually (Fig. 6A). Surprisingly, either getting rid of maternal increased *eef1a1l2* in M*nanog*,M*eef1a1l2* embryos, or eliminating both maternal and zygotic increased *eef1a1l2* in M*nanog*,MZ*eef1a1l2* embryos, could effectively rescue the developmental defects of M*nanog* (Fig. 6A). M*nanog*,M*eef1a1l2* and M*nanog*,MZ*eef1a1l2* embryos both exhibited ameliorated epiboly movement at gastrulation stage and improved axial formation except for the telencephalon defect at prim stage. However, M*nanog*,Z*eef1a1l2* embryos only lacking the

Development (2022) 149, dev201213. doi:10.1242/dev.201213

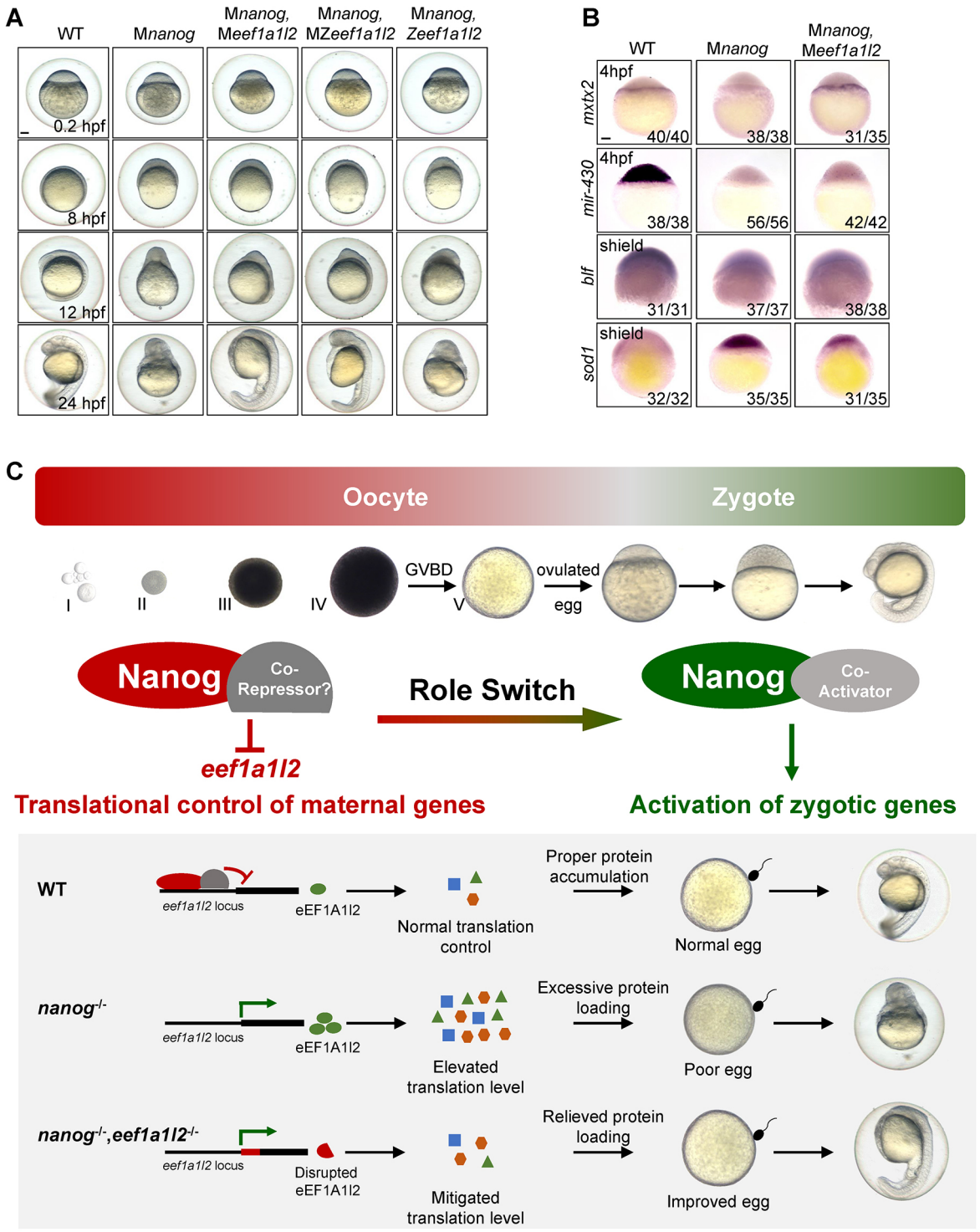

Fig. 6. Maternal depletion of *eef1a1l2* rescues the early embryonic defects of the *nanog* mutant. (A) Phenotype of WT, M*nanog*, M*nanog*,M*eef1a1l2*, M*nanog*,MZ*eef1a1l2* and M*nanog*,Z*eef1a1l2* embryos at 0.2, 8, 12 and 24 hpf. Scale bar: 100 µm. (B) Detection of *mxtx2*, *mir-430* precursor, *blf* and *sod1* in WT, M*nanog* and M*nanog*,M*eef1a1l2* embryos by WISH at the indicated stages. Scale bar: 100 µm. (C) Proposed model of Nanog function in oogenesis and early embryogenesis of zebrafish. Top: Nanog acts as a transcriptional repressor to suppress the expression of *eef1a1l2* and maintain the correct translation level of maternal mRNAs during oocyte development. Then, Nanog switches to a transcriptional activator to prime ZGA in zygotes. Bottom: In WT oocytes, Nanog inhibits the transcription of *eef1a1l2* and maintains the proper level of global translation, ensuring appropriate amounts of proteins are expressed. Good egg quality and normal embryonic development is thus guaranteed. In the absence of maternal *nanog* (*nanog*$^{-/-}$), the balance of global translation is destroyed. Elevated translation results in excessive protein loading, leading to poor egg quality and failure of embryogenesis. In *nanog* and *eef1a1l2* double-mutant oocytes (*nanog*$^{-/-}$,*eef1a1l2*$^{-/-}$), the global translation level is mitigated owing to the absence of eEF1A1l2, protein overloading is relieved and egg quality is also improved, thereby promoting a better embryonic morphology formation. Representative images shown in the schematic include data also shown in Figs 4G and 6A.

Development (2022) 149, dev201213. doi:10.1242/dev.201213

zygotic *eef1a1l2* exhibited a similar phenotype as M*nanog* (Fig. 6A), indicating that the maternally provided *eef1a1l2* mRNA in M*nanog*,Z*eef1a1l2* still led to developmental failure. In summary, the M*nanog*,M*eef1a1l2* or M*nanog*,MZ*eef1a1l2* embryos displayed rescued early embryonic development only if *eef1a1l2* was completely disrupted in the *nanog* mutant oocytes. These data indicate that the maternal activation of *eef1a1l2* in *nanog* mutant oocytes not only leads to oocyte maturation defects, but also results in early developmental defects of M*nanog* embryos.

Furthermore, we investigated the rescue effects using a set of molecular markers representing different functions of Nanog in early development. Several studies have proved that maternal Nanog directly activates *mxtx2* to regulate endoderm and extra-embryonic formation through the Nanog-*mxtx2*-Nodal pathway (Xu et al., 2012; Gagnon et al., 2018; Veil et al., 2018).We confirmed that expression of *mxtx2* was absent in M*nanog*, but the disappearance of *mxtx2* transcripts could be restored in M*nanog*,M*eef1a1l2* (Fig. 6B, Fig. S6A). During zebrafish ZGA, together with Pou5f3 and SoxB1, maternal Nanog initiates the transcription of the first major wave of zygotic genes and directly activates microRNA miR-430; maternal mRNAs are then cleared by miR-430 post-ZGA (Giraldez et al., 2006; Lee et al., 2013). Expression of the zygotic genes miR-430 and *blf* failed to be activated, and the maternal mRNA *sod1*, which is targeted by miR-430, also failed to be removed post-ZGA in M*nanog* (Fig. 6B, Fig. S5B-D). In contrast to the rescue of *mxtx2* expression, the defects of ZGA and maternal mRNA clearance could not be rescued in M*nanog*,M*eef1a1l2* embryos (Fig. 6B, Fig. S5B-D). These results illustrate that, during oogenesis, maternal Nanog safeguards oocyte development by suppression of activation of *eef1a1l2* as a transcriptional repressor, and during early embryogenesis the transcriptional suppression of *eef1a1l2* by Nanog is mainly required for transcription initiation of *mxtx2* and yolk syncytial layer formation.

All these results helped us to decipher a picture of molecular regulatory mechanisms during oogenesis and early embryonic development (Fig. 6C). During WT oogenesis, Nanog acts as a transcriptional repressor, with certain co-repressors, and directly inhibits the transcription of the eukaryotic translation elongation factor *eef1a1l2*, contributing to translational control in oocytes. After fertilization, Nanog acts as a transcriptional activator, together with Pou5f3 and SoxB1, to initiate ZGA. In oocytes produced by *nanog*$^{-/-}$ females, the transcriptional inhibition of *eef1a1l2* is absent, and ectopic maternal proteins are translated and accumulated, thus inducing ER stress and excessive UPR, leading to oocyte developmental defects. Fertilized embryos derived from the *nanog*$^{-/-}$ defective eggs fail to undergo normal gastrulation. In oocytes produced by *nanog*$^{-/-}$,*eef1a1l2*$^{-/-}$ females, however, the translation level of maternal mRNAs is mitigated owing to the lack of functional eEF1A1l2, and ER stress and UPR are alleviated, therefore leading to normal oogenesis. Therefore, it is likely that Nanog shifts from acting as a transcriptional repressor to a transcription activator during the oocyte-to-zygote transition, with both of these functions being essential for early embryogenesis.

DISCUSSION

The function of Nanog at early embryonic developmental stages has been well characterized in previous studies (Veil et al., 2018, 2019; He et al., 2020; Pálfy et al., 2020). However, as a maternally expressed gene, its role in oocyte development and maturation is still unknown. In this study, we demonstrate that zebrafish Nanog is essential for oocyte development and maturation, and has a lasting effect on early embryogenesis. Loss of maternal Nanog causes impaired oocyte maturation, deficient egg activation and early embryo developmental failure. Mechanistically, Nanog transcriptionally represses the expression of the translation elongation factor *eef1a1l2* to maintain a relative translational control state during oocyte development. In contrast, in *nanog* mutant oocytes, ectopic transcriptional activation of *eef1a1l2* elevates global translation activity and causes ER stress and UPR. Depletion of *eef1a1l2* rescues the oogenesis defects and embryonic development defects of the *nanog* mutant. Taken together, our results delineate the mechanisms underlying a general role of Nanog as a translational repressor during oogenesis.

Maternal mRNAs synthesized in the oocyte initiate the development of future generations. Some maternal mRNAs are either somatic or germline determinants and must be translationally repressed until embryogenesis (Richter and Lasko, 2011; Flora et al., 2018). A long-recognized mechanism of translational regulation during oocyte development acts by controlling mRNA poly(A)-tail length (Richter, 2007; Weill et al., 2012). The observation of short poly(A) tails in oocytes led to the proposal that short poly(A) tails help mask maternal mRNAs and promote translational repression. Certain mRNAs, such as *c-mos* and several cyclin genes, are then targeted for cytoplasmic polyadenylation, and the lengthened poly(A) tails in turn cause translational upregulation of these mRNAs during oocyte maturation in *Xenopus* (Mcgrew et al., 1989; Sheets et al., 1994; Barkoff et al., 1998). In our study, however, *cyclin B1* and *zp3b* mRNAs were still translationally activated in *nanog* mutant early oocytes, although they were translationally silent in WT early oocytes, suggesting that their poly(A) tail should be relatively short. The increased translational level of Cyclin B1 and Zp3b in *nanog* mutant oocytes was suppressed in *nanog* and *eef1a1l2* double mutant oocyte (Fig. S5A-D), assuming that the changes in the translation level of maternal mRNA in *nanog*-null oocytes are mainly dependent on the transcriptional activation of *eef1a1l2* rather than on the size of the poly(A) tail of mRNAs. Another widely studied mechanism of translational regulation acts through sequence-specific regulators, mostly RNA-binding proteins, which post-transcriptionally maintain translational repression of mRNAs containing targeted cis-regulatory elements in gametogenesis and early embryogenesis (Tadros et al., 2007; Sha et al., 2017), as has been shown for some germline mRNAs, such as *oskar*, *pgc* and *nanos*, during oocyte maturation in *Drosophila* (Smibert et al., 1996; Kugler and Lasko, 2009; Flora et al., 2018). However, different from these mechanisms, in this study we demonstrated a translational control mechanism mediated by Nanog, which transcriptionally inhibits the expression of a translational elongation factor, eEF1A1l2, and controls the maternal mRNA translational activity during oogenesis. The translational control mediated by Nanog is relatively a global one, and does not depend on the specificity of mRNA sequence and on the size of the poly(A) tail of mRNAs. Thus, this study reveals a mechanism of translational control regulated by Nanog to promote oogenesis and early embryonic development.

Genes that are not transcribed in oocytes and mature eggs are considered as non-maternal genes or zygotic genes. In theory, the transcription of non-maternal genes should be suppressed in oocytes to safeguard oocyte development and maturation and early embryonic patterning. Abnormal activation and expression of non-maternal genes will change the cell fate of the oocyte, impair oocyte development, and even lead to oocyte apoptosis. Based on the expression pattern of *eef1a1l2* during oogenesis and early embryonic development in WT (Fig. 3B,C, Fig. S3), we found that *eef1a1l2* has no maternal expression in oocytes, indicating that

Development (2022) 149, dev201213. doi:10.1242/dev.201213

eef1a1l2 is a non-maternal gene and is not employed during oogenesis. However, *eef1a1l2* is precociously transcribed in *nanog* mutant oocytes, leading to overactivation of global translational activity, which in turn impairs oocyte development and maturation. This finding implies that Nanog may protect oogenesis and early embryogenesis by suppressing the transcriptional activation of non-maternal genes.

Studies in human and mouse embryonic stem cells have shown that Nanog acts as both a transcriptional activator and a transcriptional repressor (Boyer et al., 2005; Liang et al., 2008). As a transcriptional activator, Nanog, in cooperation with Pou5f3 and Sox2, transcriptionally activates the expression of genes responsible for stem cell self-renewal and maintenance of pluripotency, whereas as a transcriptional repressor Nanog is associated with repression complexes and transcriptionally represses the expression of genes related to differentiation and development. In this study, we conclude that Nanog acts as a transcriptional repressor to suppress the transcription of *eef1a1l2*, and speculate that Nanog safeguards oogenesis by suppressing *eef1a1l2* during oocyte development in zebrafish. However, Nanog is known to act as a transcription activator in ZGA and shapes the embryo during zebrafish gastrulation. For instance, Nanog initiates ZGA together with Pou5f3 and SoxB1, and miR-430 is directly activated by Nanog and is responsible for clearance of maternal mRNA during MZT (Lee et al., 2013). Further studies have shown that Nanog binds to the high nucleosome affinity regions center and synergistically opens chromatin along with Pou5f3 and Sox19b, priming genes for activity during ZGA in zebrafish (Veil et al., 2019; Pálfy et al., 2020). Nanog directly activates *mxtx2* and regulates the formation of extra-embryonic tissue and embryonic architecture (Xu et al., 2012; Gagnon et al., 2018; Veil et al., 2018). Quantitative imaging also shows that Nanog cooperates with Pou5f3 to promote ventral fate (Perez-Camps et al., 2016). These studies illustrate that Nanog switches from transcriptional repressor to transcriptional activator during the oocyte-to-zygote transition. As a homeodomain protein, Nanog binds to target genes at the homeobox domain, but the question of which repressive partner interacts with Nanog to exert the gene silencing function in oocytes needs further investigation

MATERIALS AND METHODS

Zebrafish maintenance

All the zebrafish used in this study were maintained and raised as previously described (Westerfield, 1995) at the China Zebrafish Resource Center of the National Aquatic Biological Resource Center (CZRC-NABRC, Wuhan, China; http://zfish.cn). WT embryos were collected by natural spawning from the AB strain. Oocyte developmental stages were classified according to previous studies (Selman et al., 1993; Lubzens et al., 2010). Developmental stages of mutant embryos were indirectly determined by observation of WT embryos born at the same time and incubated under identical conditions. Experiments involving zebrafish were performed under the approval of the Institutional Animal Care and Use Committee of the Institute of Hydrobiology, Chinese Academy of Sciences, under protocol number IHB2014-006.

Generation of *nanog* and *eef1a1l2* double mutants

M*nanog* was generated by crossing *nanog*$^{-/-}$ females with WT males as previously described (He et al., 2015, 2020). The *eef1a1l2* mutant was generated in a *nanog* mutant background using CRISPR/Cas9. The gRNA target and PAM sequence (underlined) of *eef1a1l2* was 5′-GGCCACCTCATTTACAGTGTGG-3′; pT3TS-zCas9 was used for Cas9 mRNA transcription; capped Cas9 mRNA was generated using the T3 mMessage Machine kit (AM1344, Ambion). gRNA was generated by *in vitro* transcription using T7 RNA polymerase (Promega). Cas9 mRNA and gRNA were co-injected into embryos created by crossing *nanog*$^{+/-}$ females and *nanog*$^{-/-}$ males at the one-cell stage. M*nanog*/M*eef1a1l2* was obtained by crossing *nanog*$^{-/-}$,*eef1a1l2*$^{-/-}$ females with WT males. The primers used for mutant screening are listed in Table S2.

Morphological analysis of ovaries and oocytes

After anesthesia by immersion in 0.16 mg/ml tricaine methanesulfonate (MS-222), we dissected the intact gonadal tissues from WT, *nanog*$^{-/-}$ and *nanog*$^{-/-}$,*eef1a1l2*$^{-/-}$ adult zebrafish (4 months post-fertilization) and calculated the GSI (gonad weight/body weight×100%). For embryos, chorion elevation distance and oocyte diameter were measured at 15 mpf using ImageJ. Oocyte diameter was measured as the longest distance in the vertical direction of the animal-vegetal axis. Chorion diameter was considered to be the longest length of chorion when it was fully inflated.

Follicle isolation, *in vitro* culture and GVBD assay

Ovaries were dissected from adult females and transferred into oocyte sorting medium, made from 90% Leibovitz's L-15 medium (Gibco) and 10% fetal bovine serum (Boehringer Ingelheim) with 100 µg/ml Penicillin-Streptomycin (Gibco). Follicles (follicle-enclosed oocytes) were manually separated and divided into five groups based on oocyte size and vitellogenic state: primary growth stage (stage I), previtellogenic stage (stage II), vitellogenic stage (stage III), full-growth stage (stage IV) and mature oocytes (follicles after GVBD *in vitro*; stage V). Ovulated maturation oocytes were defined as eggs. Different stages of follicles were gently separated using two tweezers in a dish covered with 1% agarose.

Dissociated stage IV follicles were transferred into oocyte culture medium (OCM) by gentle pipetting. OCM was made from 90% Leibovitz's L-15 medium and 10% fetal bovine serum with 1 µg/ml DHP (Cayman Chemical). Sorted oocytes were cultured at 28°C for 2 h according to a previous study (Nair et al., 2013). GVBD rates were determined in a unified standard by ImageJ. The concentrations of different inhibitors added to OCM were: 4EGI-1 (25 ng/µl, Santa Cruz Biotechnology), ISRIB (5 µM, Selleck), GSK2606414 (50 nM, Selleck).

CG staining

Ovulated eggs at 10 mpa in water were collected and fixed with 4% paraformaldehyde (PFA) overnight prior to further steps. CGs were visualized by staining embryos with 50 µg/ml FITC-conjugated *Maclura pomifera* agglutinin (Vector Laboratories, FL-1341) as previously described (Mei et al., 2009).

SDS-PAGE and Coomassie staining

SDS-PAGE and Coomassie staining were performed following the established protocol (Schägger, 2006). To obtain yolk protein, ten follicles at indicated stage were lysed in 500 µl TNE buffer, made from 10 mM Tris-HCl (pH 7.4), 150 mM NaCl, 5 mM EDTA and 1% Triton X-100; 10 µl lysate was loaded for SDS-PAGE and Coomassie staining as previously described (Sun et al., 2018). Intensity measurement was carried out using ImageJ.

Western blot analysis

GFP protein was purchased form DIA-AN Biotechnology and 20 pg of GFP protein per embryo was co-injected at the one-cell stage. Injected embryos or dissected ovaries were homogenized using RIPA (P0013B, Beyotime). Western blot was carried out as previously described (Ye et al., 2019). Primary antibodies and dilutions for western blot were: GAPDH (2058, DIA-AN, 1:3000), mCherry (BE2026, Easybio, 1:2000), GFP (2057, DIA-AN, 1:2000), Hspa5 (11587-1-AP, Proteintech, 1:2000), Ddit3 (AC532, Beyotime, 1:2000), S6 (2217S, CST, 1:1000), pS6 (2215S, CST, 1:1000), Cyclin B1 (A2056, ABclonal, 1:1500), Zp3b (A13156, ABclonal, 1:1500).

RNA-seq and analysis

Total RNA of ovulated eggs of WT and *nanog* homozygous were extracted using TRIzol Reagent (Invitrogen) and mRNA was enriched using oligo-dT

Development (2022) 149, dev201213. doi:10.1242/dev.201213

magnetic beads. First-strand cDNAs (from purified mRNA) were synthesized using random hexamers. The PCR-amplified cDNA was purified using AMPure XP beads, then 1 µl cDNA was validated using an Agilent 2100 Bioanalyzer. Sequencing libraries were generated using the Illumina TruSeq RNA sample preparation kit v2 according to the manufacturer's recommendations. Clustered library preparations were sequenced on an Illumina HiSeq 2000 machine and 100 bp single-end reads were generated. Clean reads, with low quality reads removed from the raw data, were mapped to the zebrafish GRCz10 reference genome using TopHat2 (Kim et al., 2013). HTSeq v0.6.1 was used to count the read numbers mapped to each gene. Then, the RPKM of each gene was calculated to determine gene expression levels (Trapnell et al., 2010). Differential expression analysis was performed using DESeq (Anders and Huber, 2010). Genes with an adjusted $P<0.05$ as calculated by DESeq were considered differentially expressed.

Proteomics

Ovulated eggs of WT and *nanog* homozygous were pooled and homogenized for quantitative proteomic analysis. The iTRAQ analysis was performed as previously described (Miao et al., 2017). The UniPort proteome sequence for *Danio rerio* was used for database searching.

ChIP-PCR

ChIP assays were performed with a ChIP assay kit (Cell Signaling Technology) as described (Wei et al., 2014). Briefly, two ovaries of *Tg*(CMV:*nanog-myc*) at 6 mpf were dissected and lysed for ChIP assay. Immunoprecipitation was carried out using an anti-Myc antibody (Cell Signaling Technology). Immunoprecipitation of genomic *eef1a1l2* in immunoprecipitated chromatin was detected by PCR. Primers specific for the *eef1a1l2* promoter region were used and the sequences are listed in Table S2. The exon of the ribosomal protein *rpl5b* served as a negative control, with primers 5′-GGGGATGAGTTCAATGTGGAG-3′ (forward) and 5′-CGAACACCTTATTGCCAGTAG-3′ (reverse), as described (Belting et al., 2011).

TEM analysis

Isolated stage I/II follicles from different genotypic ovaries were collected into a test tube and fixed with 100 µl 2.5% glutaraldehyde at 4°C overnight. Sample preparation for TEM was carried out according to a previously described protocol (Zhang et al., 2022) and observed under a Hitachi HT7700 transmission electron microscope.

In situ hybridization

PCR-amplified sequences of genes of interest were used as templates for the synthesis of an antisense RNA probe, labeled with digoxigenin-linked nucleotides. Whole-mount *in situ* hybridization (WISH) on embryos was performed as described previously (Thisse and Thisse, 2008). For *in situ* hybridization on frozen section, adult ovaries were stripped and embedded in Optimal Cutting Temperature compound (O.C.T., Sakura Finetek) and sectioned at 10 µm. The procedures of hybridization followed a previous study (Zhang et al., 2020).

Immunofluorescence

For whole-mount immunofluorescence, embryos were collected and fixed in 4% PFA overnight at 4°C. For immunofluorescence on cryosections, sections were prepared as for *in situ* hybridization and fixed in 4% PFA for 20 min at room temperature. Embryos and slides were immunostained as described in previous studies (He et al., 2020; Zhang et al., 2022). Primary antibodies and dilutions were: cleaved Caspase 3 (#9661, Cell Signaling Technology, 1:1000), Myc (#2276, Cell Signaling Technology, 1:1000).

RT-qPCR

Total RNA was extracted from samples using TRIzol (Invitrogen). RNA was reverse-transcribed with the PrimeScript RT reagent kit (Thermo Fisher Scientific) and the relative abundance of target mRNAs was examined with gene-specific primers. *gapdh* was used as a normalization control. Sequences of PCR primers are listed in Table S2. RT-qPCR was performed using the SYBR Green Supermix from Bio-Rad on a Bio-Rad CFX96 detection system.

Stem-loop RT-PCR of miR-430a

Stem-loop RT-PCR was performed to quantify the expression of miR-430a as previously described (Chen et al., 2005). Total RNAs were reversely transcribed using miR-430a-specific primers and U6 was used as internal control. The PCR primers of miR-430a and U6 used in this study have been described in a previous study (He et al., 2020).

TUNEL assay

Ovaries were dissected from WT and *nanog*$^{-/-}$ adult fish at 4 months post-fertilization and cryosections were prepared as for *in situ* hybridization. The samples were sectioned at 10 µm thickness. The TUNEL cell death assay was performed using the In Situ Cell Death Detection Kit (Roche) according to the manufacturer's instructions. Images were obtained using a laser scanning confocal microscope (Leica SP8).

Statistical analysis

GraphPad Prism 8.3.0 software was used for statistical analyses and statistical graphs. Significance of differences between means was analyzed using unpaired, one-tailed Student's *t*-tests. Sample sizes are indicated in the figure legends. Data are shown as mean±s.d. and *P*-values indicated as follows: $*P<0.05$, $**P<0.01$, $***P<0.001$ 0.001. 'NS' indicates no significant difference.

Acknowledgements

We thank other members of the Sun laboratory for method advice and manuscript discussions, and Linglu Li from the China Zebrafish Resource Center for assistance with raising fish.

Competing interests

The authors declare no competing or financial interests.

Author contributions

Conceptualization: M.H., S.J., Y.S.; Methodology: M.H., S.J.; Formal analysis: M.H., S.J.; Investigation: M.H.; Resources: H.W.; Data curation: R.Z.; Writing - original draft: M.H.; Writing - review & editing: D.Y., Y.S.; Supervision: Y.S.; Project administration: M.H., Y.S.; Funding acquisition: M.H., Y.S.

Funding

This work was supported by National Natural Science Foundation of China (32025037, 32273134 and 31702323), the Strategic Priority Research Program of the Chinese Academy of Sciences (XDA24010108), the Ministry of Science and Technology of the People's Republic of China (2018YFA0801000 and NK2022010207) and the State Key Laboratory of Freshwater Ecology and Biotechnology (2019FBZ05).

Data availability

RNA-seq data in this study have been deposited in Science Data Bank (doi:10.57760/sciencedb.04575) and in BioProject with accession number PRJNA633216. The mass spectrometry proteomics data have been deposited to the ProteomeXchange Consortium (http://proteomecentral.proteomexchange.org) via the iProX partner repository with the dataset identifier PXD036250.

Peer review history

The peer review history is available online at https://journals.biologists.com/dev/lookup/doi/10.1242/dev.201213.reviewer-comments.pdf

References

Anders, S. and Huber, W. (2010). Differential expression analysis for sequence count data. *Genome Biol.* **11**, R106. doi:10.1186/gb-2010-11-10-r106

Barkoff, A., Ballantyne, S. and Wickens, M. (1998). Meiotic maturation in Xenopus requires polyadenylation of multiple mRNAs. *EMBO J.* **17**, 3168-3175. doi:10.1093/emboj/17.11.3168

Belting, H.-G., Wendik, B., Lunde, K., Leichsenring, M., Mössner, R., Driever, W. and Onichtchouk, D. (2011). Pou5f1 contributes to dorsoventral patterning by positive regulation of vox and modulation of fgf8a expression. *Dev. Biol.* **356**, 323-336. doi:10.1016/j.ydbio.2011.05.660

Biever, A., Valjent, E. and Puighermanal, E. (2015). Ribosomal protein S6 phosphorylation in the nervous system: from regulation to function. *Front. Mol. Neurosci.* **8**, 75. doi:10.3389/fnmol.2015.00075
Boyer, L. A., Lee, T. I., Cole, M. F., Johnstone, S. E., Levine, S. S., Zucker, J. P., Guenther, M. G., Kumar, R. M., Murray, H. L., Jenner, R. G. et al. (2005). Core transcriptional regulatory circuitry in human embryonic stem cells. *Cell* **122**, 947-956. doi:10.1016/j.cell.2005.08.020
Chen, C., Ridzon, D. A., Broomer, A. J., Zhou, Z., Lee, D. H., Nguyen, J. T., Barbisin, M., Xu, N. L., Mahuvakar, V. R., Andersen, M. R. et al. (2005). Real-time quantification of microRNAs by stem-loop RT-PCR. *Nucleic Acids Res.* **33**, e179. doi:10.1093/nar/gni178
Dahanukar, A. and Wharton, R. P. (1996). The Nanos gradient in Drosophila embryos is generated by translational regulation. *Genes Dev.* **10**, 2610-2620. doi:10.1101/gad.10.20.2610
Dosch, R., Wagner, D. S., Mintzer, K. A., Runke, G., Wiemelt, A. P. and Mullins, M. C. (2004). Maternal control of vertebrate development before the midblastula transition: mutants from the Zebrafish I. *Dev. Cell* **6**, 771-780. doi:10.1016/j.devcel.2004.05.002
Evans, T. C. and Hunter, C. P. (2005). Translational control of maternal RNAs. In *WormBook*, 1-11. doi:10.1895/wormbook.1.34.1
Flora, P., Wong-Deyrup, S. W., Martin, E. T., Palumbo, R. J., Nasrallah, M., Oligney, A., Blatt, P., Patel, D., Fuchs, G. and Rangan, P. (2018). Sequential regulation of maternal mRNAs through a conserved cis-acting element in their 3′ UTRs. *Cell Rep.* **25**, 3828-3843.e9. doi:10.1016/j.celrep.2018.12.007
Gagnon, J. A., Obbad, K. and Schier, A. F. (2018). The primary role of zebrafish nanog is in extra-embryonic tissue. *Development* **145**, dev147793. doi:10.1242/dev.147793
Giraldez, A. J., Mishima, Y., Rihel, J., Grocock, R. J., Van Dongen, S., Inoue, K., Enright, A. J. and Schier, A. F. (2006). Zebrafish MiR-430 promotes deadenylation and clearance of maternal mRNAs. *Science* **312**, 75-79. doi:10.1126/science.1122689
Gosden, R. and Lee, B. (2010). Portrait of an oocyte: our obscure origin. *J. Clin. Investig.* **120**, 973-983. doi:10.1172/JCI41294
He, M.-D., Zhang, F.-H., Wang, H.-L., Wang, H.-P., Zhu, Z.-Y. and Sun, Y.-H. (2015). Efficient ligase 3-dependent microhomology-mediated end joining repair of DNA double-strand breaks in zebrafish embryos. *Mutat. Res.* **780**, 86-96. doi:10.1016/j.mrfmmm.2015.08.004
He, M., Zhang, R., Jiao, S., Zhang, F., Ye, D., Wang, H. and Sun, Y. (2020). Nanog safeguards early embryogenesis against global activation of maternal β-catenin activity by interfering with TCF factors. *PLoS Biol.* **18**, e3000561. doi:10.1371/journal.pbio.3000561
Hetz, C. (2012). The unfolded protein response: controlling cell fate decisions under ER stress and beyond. *Nat. Rev. Mol. Cell Biol.* **13**, 89-102. doi:10.1038/nrm3270
Iurlaro, R. and Muñoz-Pinedo, C. (2016). Cell death induced by endoplasmic reticulum stress. *FEBS J.* **283**, 2640-2652. doi:10.1111/febs.13598
Jamieson-Lucy, A. and Mullins, M. C. (2019). The vertebrate Balbiani body, germ plasm, and oocyte polarity. *Curr. Top. Dev. Biol.* **135**, 1-34. doi:10.1016/bs.ctdb.2019.04.003
Kaufman, R. J. (2002). Orchestrating the unfolded protein response in health and disease. *J. Clin. Invest.* **110**, 1389-1398. doi:10.1172/JCI0216886
Kim, D., Pertea, G., Trapnell, C., Pimentel, H., Kelley, R. and Salzberg, S. L. (2013). TopHat2: accurate alignment of transcriptomes in the presence of insertions, deletions and gene fusions. *Genome Biol.* **14**, R36-R36. doi:10.1186/gb-2013-14-4-r36
Kim-Ha, J., Kerr, K. and Macdonald, P. M. (1995). Translational regulation of oskar mRNA by bruno, an ovarian RNA-binding protein, is essential. *Cell* **81**, 403-412. doi:10.1016/0092-8674(95)90393-3
Kotani, T., Yasuda, K., Ota, R. and Yamashita, M. (2013). Cyclin B1 mRNA translation is temporally controlled through formation and disassembly of RNA granules. *J. Cell Biol.* **202**, 1041-1055. doi:10.1083/jcb.201302139
Kugler, J.-M. and Lasko, P. (2009). Localization, anchoring and translational control of oskar, gurken, bicoid and nanos mRNA during Drosophila oogenesis. *Fly (Austin)***3**, 15-28. doi:10.4161/fly.3.1.7751
Lee, M. T., Bonneau, A. R., Takacs, C. M., Bazzini, A. A., DiVito, K. R., Fleming, E. S. and Giraldez, A. J. (2013). Nanog, Pou5f1 and SoxB1 activate zygotic gene expression during the maternal-to-zygotic transition. *Nature* **503**, 360-364. doi:10.1038/nature12632
Li, J., Gao, L.-Y., Colorni, A., Ucko, M., Fang, S. and Du, S. J. (2015). A transgenic zebrafish model for monitoring xbp1 splicing and endoplasmic reticulum stress in vivo. *Mech. Dev.* **137**, 33-44. doi:10.1016/j.mod.2015.04.001
Liang, J., Wan, M., Zhang, Y., Gu, P., Xin, H., Jung, S. Y., Qin, J., Wong, J., Cooney, A. J., Liu, D. et al. (2008). Nanog and Oct4 associate with unique transcriptional repression complexes in embryonic stem cells. *Nat. Cell Biol.* **10**, 731-739. doi:10.1038/ncb1736
Loh, Y.-H., Wu, Q., Chew, J.-L., Vega, V. B., Zhang, W., Chen, X., Bourque, G., George, J., Leong, B., Liu, J. et al. (2006). The Oct4 and Nanog transcription network regulates pluripotency in mouse embryonic stem cells. *Nat. Genet.* **38**, 431-440. doi:10.1038/ng1760
Lubzens, E., Young, G., Bobe, J. and Cerdà, J. (2010). Oogenesis in teleosts: how eggs are formed. *Gen. Comp. Endocrinol.* **165**, 367-389. doi:10.1016/j.ygcen.2009.05.022
Marlow, F. L. and Mullins, M. C. (2008). Bucky ball functions in Balbiani body assembly and animal-vegetal polarity in the oocyte and follicle cell layer in zebrafish. *Dev. Biol.* **321**, 40-50. doi:10.1016/j.ydbio.2008.05.557
Mcgrew, L. L., Dworkin-Rastl, E., Dworkin, M. B. and Richter, J. D. (1989). Poly(A) elongation during Xenopus oocyte maturation is required for translational recruitment and is mediated by a short sequence element. *Genes Dev.* **3**, 803-815. doi:10.1101/gad.3.6.803
Mei, W., Lee, K. W., Marlow, F. L., Miller, A. L. and Mullins, M. C. (2009). hnRNP I is required to generate the Ca^{2+} signal that causes egg activation in zebrafish. *Development* **136**, 3007-3017. doi:10.1242/dev.037879
Meyuhas, O. (2015). Ribosomal protein S6 phosphorylation: four decades of research. *Int. Rev. Cell Mol. Biol.* **320**, 41-73. doi:10.1016/bs.ircmb.2015.07.006
Miao, L., Yuan, Y., Cheng, F., Fang, J., Zhou, F., Ma, W., Jiang, Y., Huang, X., Wang, Y., Shan, L. et al. (2017). Translation repression by maternal RNA binding protein Zar1 is essential for early oogenesis in zebrafish. *Development* **144**, 128-138. doi:10.1242/dev.144642
Mitsui, K., Tokuzawa, Y., Itoh, H., Segawa, K., Murakami, M., Takahashi, K., Maruyama, M., Maeda, M. and Yamanaka, S. (2003). The homeoprotein Nanog is required for maintenance of pluripotency in mouse epiblast and ES cells. *Cell* **113**, 631-642. doi:10.1016/S0092-8674(03)00393-3
Moerke, N. J., Aktas, H., Chen, H., Cantel, S., Reibarkh, M. Y., Fahmy, A., Gross, J. D., Degterev, A., Yuan, J., Chorev, M. et al. (2007). Small-molecule inhibition of the interaction between the translation initiation factors eIF4E and eIF4G. *Cell* **128**, 257-267. doi:10.1016/j.cell.2006.11.046
Nair, S., Lindeman, R. E. and Pelegri, F. (2013). In vitro oocyte culture-based manipulation of zebrafish maternal genes. *Dev. Dyn.* **242**, 44-52. doi:10.1002/dvdy.23894
Nakamura, A., Amikura, R., Hanyu, K. and Kobayashi, S. (2001). Me31B silences translation of oocyte-localizing RNAs through the formation of cytoplasmic RNP complex during Drosophila oogenesis. *Development* **128**, 3233-3242. doi:10.1242/dev.128.17.3233
Oyadomari, S. and Mori, M. (2004). Roles of CHOP/GADD153 in endoplasmic reticulum stress. *Cell Death Differ.* **11**, 381-389. doi:10.1038/sj.cdd.4401373
Pálfy, M., Schulze, G., Valen, E. and Vastenhouw, N. L. (2020). Chromatin accessibility established by Pou5f3, Sox19b and Nanog primes genes for activity during zebrafish genome activation. *PLoS Genet.* **16**, e1008546. doi:10.1371/journal.pgen.1008546
Perez-Camps, M., Tian, J., Chng, S. C., Sem, K. P., Sudhaharan, T., Teh, C., Wachsmuth, M., Korzh, V., Ahmed, S. and Reversade, B. (2016). Quantitative imaging reveals real-time Pou5f3-Nanog complexes driving dorsoventral mesendoderm patterning in zebrafish. *eLife* **5**, e11475. doi:10.7554/eLife.11475
Petrachkova, T., Wortinger, L. A., Bard, A. J., Singh, J., Warga, R. M. and Kane, D. A. (2019). Lack of Cyclin B1 in zebrafish causes lengthening of G2 and M phases. *Dev. Biol.* **451**, 167-179. doi:10.1016/j.ydbio.2019.03.014
Piqué, M., López, J. M., Foissac, S., Guigó, R. and Méndez, R. (2008). A combinatorial code for CPE-mediated translational control. *Cell* **132**, 434-448. doi:10.1016/j.cell.2007.12.038
Rao, R. V. and Bredesen, D. E. (2004). Misfolded proteins, endoplasmic reticulum stress and neurodegeneration. *Curr. Opin. Cell Biol.* **16**, 653-662. doi:10.1016/j.ceb.2004.09.012
Richter, J. D. (2007). CPEB: a life in translation. *Trends Biochem. Sci.* **32**, 279-285. doi:10.1016/j.tibs.2007.04.004
Richter, J. D. and Lasko, P. (2011). Translational control in oocyte development. *Cold Spring Harb. Perspect. Biol.* **3**, a002758. doi:10.1101/cshperspect.a002758
Sasikumar, A. N., Perez, W. B. and Kinzy, T. G. (2012). The many roles of the eukaryotic elongation factor 1 complex. *Wiley Interdiscipl. Rev. RNA* **3**, 543-555. doi:10.1002/wrna.1118
Schägger, H. (2006). Tricine-SDS-PAGE. *Nat. Protoc.* **1**, 16-22. doi:10.1038/nprot.2006.4
Schröder, M. and Kaufman, R. J. (2005). ER stress and the unfolded protein response. *Mutat. Res.* **569**, 29-63. doi:10.1016/j.mrfmmm.2004.06.056
Selman, K., Wallace, R. A., Sarka, A. and Qi, X. (1993). Stages of oocyte development in the zebrafish, Brachydanio rerio. *J. Morphol.* **218**, 203-224. doi:10.1002/jmor.1052180209
Sha, Q.-Q., Dai, X.-X., Dang, Y., Tang, F., Liu, J., Zhang, Y.-L. and Fan, H.-Y. (2017). A MAPK cascade couples maternal mRNA translation and degradation to meiotic cell cycle progression in mouse oocytes. *Development* **144**, 452-463. doi:10.1242/dev.144410
Sheets, M. D., Fox, C. A., Hunt, T., Vande Woude, G. and Wickens, M. (1994). The 3′-untranslated regions of c-mos and cyclin mRNAs stimulate translation by regulating cytoplasmic polyadenylation. *Genes Dev.* **8**, 926-938. doi:10.1101/gad.8.8.926
Shen, X., Ellis, R. E., Lee, K., Liu, C.-Y., Yang, K., Solomon, A., Yoshida, H., Morimoto, R., Kurnit, D. M., Mori, K. et al. (2001). Complementary signaling pathways regulate the unfolded protein response and are required for C. elegans development. *Cell* **107**, 893-903. doi:10.1016/S0092-8674(01)00612-2

Shen, X., Zhang, K. and Kaufman, R. J. (2004). The unfolded protein response – a stress signaling pathway of the endoplasmic reticulum. *J. Chem. Neuroanat.* **28**, 79-92. doi:10.1016/j.jchemneu.2004.02.006

Silva, J., Nichols, J., Theunissen, T. W., Guo, G., van Oosten, A. L., Barrandon, O., Wray, J., Yamanaka, S., Chambers, I. and Smith, A. (2009). Nanog is the gateway to the pluripotent ground state. *Cell* **138**, 722-737. doi:10.1016/j.cell.2009.07.039

Smibert, C. A., Wilson, J. E., Kerr, K. and Macdonald, P. M. (1996). Smaug protein represses translation of unlocalized nanos mRNA in the Drosophila embryo. *Genes Dev.* **10**, 2600-2609. doi:10.1101/gad.10.20.2600

Smibert, C. A., Lie, Y. S., Shillinglaw, W., Henzel, W. J. and Macdonald, P. M. (1999). Smaug, a novel and conserved protein, contributes to repression of nanos mRNA translation in vitro. *RNA* **5**, 1535-1547. doi:10.1017/S1355838299991392

Snee, M., Benz, D., Jen, J. and Macdonald, P. M. (2008). Two distinct domains of Bruno bind specifically to the oskar mRNA. *RNA Biol.* **5**, 49-57. doi:10.4161/rna.5.1.5735

Sun, J., Yan, L., Shen, W. and Meng, A. (2018). Maternal Ybx1 safeguards zebrafish oocyte maturation and maternal-to-zygotic transition by repressing global translation. *Development* **145**, dev166587. doi:10.1242/dev.166587

Tadros, W., Goldman, A. L., Babak, T., Menzies, F., Vardy, L., Orr-Weaver, T., Hughes, T. R., Westwood, J. T., Smibert, C. A. and Lipshitz, H. D. (2007). SMAUG is a major regulator of maternal mRNA destabilization in Drosophila and its translation is activated by the PAN GU kinase. *Dev. Cell* **12**, 143-155. doi:10.1016/j.devcel.2006.10.005

Takahashi, K. and Yamanaka, S. (2006). Induction of pluripotent stem cells from mouse embryonic and adult fibroblast cultures by defined factors. *Cell* **126**, 663-676. doi:10.1016/j.cell.2006.07.024

Takahashi, K., Kotani, T., Katsu, Y. and Yamashita, M. (2014). Possible involvement of insulin-like growth factor 2 mRNA-binding protein 3 in zebrafish oocyte maturation as a novel cyclin B1 mRNA-binding protein that represses the translation in immature oocytes. *Biochem. Biophys. Res. Commun.* **448**, 22-27. doi:10.1016/j.bbrc.2014.04.020

Thisse, C. and Thisse, B. (2008). High-resolution in situ hybridization to whole-mount zebrafish embryos. *Nat. Protoc.* **3**, 59-69. doi:10.1038/nprot.2007.514

Trapnell, C., Williams, B. A., Pertea, G., Mortazavi, A., Kwan, G., van Baren, M. J., Salzberg, S. L., Wold, B. J. and Pachter, L. (2010). Transcript assembly and quantification by RNA-Seq reveals unannotated transcripts and isoform switching during cell differentiation. *Nat. Biotechnol.* **28**, 511-515. doi:10.1038/nbt.1621

Vardy, L. and Orr-Weaver, T. L. (2007). The Drosophila PNG kinase complex regulates the translation of cyclin B. *Dev. Cell* **12**, 157-166. doi:10.1016/j.devcel.2006.10.017

Veil, M., Schaechtle, M. A., Gao, M. J., Kirner, V., Buryanova, L., Grethen, R. and Onichtchouk, D. (2018). Maternal Nanog is required for zebrafish embryo architecture and for cell viability during gastrulation. *Development* **145**, dev155366. doi:10.1242/dev.155366

Veil, M., Yampolsky, L. Y., Gruning, B. and Onichtchouk, D. (2019). Pou5f3, SoxB1, and Nanog remodel chromatin on high nucleosome affinity regions at zygotic genome activation. *Genome Res.* **29**, 383-395. doi:10.1101/344168

Wang, M., Ly, M., Lugowski, A., Laver, J. D., Lipshitz, H. D., Smibert, C. A. and Rissland, O. S. (2017). ME31B globally represses maternal mRNAs by two distinct mechanisms during the Drosophila maternal-to-zygotic transition. *eLife* **6**, e27891. doi:10.7554/eLife.27891

Wei, C.-Y., Wang, H.-P., Zhu, Z.-Y. and Sun, Y.-H. (2014). Transcriptional factors smad1 and smad9 act redundantly to mediate zebrafish ventral specification downstream of smad5. *J. Biol. Chem.* **289**, 6604-6618. doi:10.1074/jbc.M114.549758

Weill, L., Belloc, E., Bava, F.-A. and Méndez, R. (2012). Translational control by changes in poly(A) tail length: recycling mRNAs. *Nat. Struct. Mol. Biol.* **19**, 577-585. doi:10.1038/nsmb.2311

Westerfield, M. (1995). *The Zebrafish Book: A Guide for the Laboratory use of Zebrafish (Danio rerio)*. Eugene, OR: M. Westerfield.

Xu, C., Fan, Z. P., Müller, P., Fogley, R., DiBiase, A., Trompouki, E., Unternaehrer, J., Xiong, F., Torregroza, I., Evans, T. et al. (2012). Nanog-like regulates endoderm formation through the Mxtx2-Nodal pathway. *Dev. Cell* **22**, 625-638. doi:10.1016/j.devcel.2012.01.003

Yarunin, A., Harris, R. E., Ashe, M. P. and Ashe, H. L. (2011). Patterning of the Drosophila oocyte by a sequential translation repression program involving the d4EHP and Belle translational repressors. *RNA Biol.* **8**, 904-912. doi:10.4161/rna.8.5.16325

Ye, D., Wang, X., Wei, C., He, M., Wang, H., Wang, Y., Zhu, Z. and Sun, Y. (2019). Marcksb plays a key role in the secretory pathway of zebrafish Bmp2b. *PLoS Genet.* **15**, e1008306. doi:10.1371/journal.pgen.1008306

Yoshida, H., Matsui, T., Yamamoto, A., Okada, T. and Mori, K. (2001). XBP1 mRNA is induced by ATF6 and spliced by IRE1 in response to ER stress to produce a highly active transcription factor. *Cell* **107**, 881-891. doi:10.1016/S0092-8674(01)00611-0

Zhang, Q., Ye, D., Wang, H., Wang, Y., Hu, W. and Sun, Y. (2020). Zebrafish cyp11c1 knockout reveals the roles of 11-ketotestosterone and cortisol in sexual development and reproduction. *Endocrinology* **161**, bqaa048. doi:10.1210/endocr/bqaa048

Zhang, F., Hao, Y., Li, X., Li, Y., Ye, D., Zhang, R., Wang, X., He, M., Wang, H., Zhu, Z. et al. (2022). Surrogate production of genome-edited sperm from a different subfamily by spermatogonial stem cell transplantation. *Sci. China Life Sci.* **65**, 969-987. doi:10.1007/s11427-021-1989-9